Monthly Notices
of the
ROYAL ASTRONOMICAL SOCIETY

MNRAS **474,** 4988–4996 (2018)
Advance Access publication 2017 December 1

doi:10.1093/mnras/stx3050

A disrupted molecular torus around Eta Carinae as seen in ^{12}CO with ALMA

Nathan Smith,[1]★ Adam Ginsburg[2,3]† and John Bally[4]

[1]*Steward Observatory, University of Arizona, 933 N. Cherry Ave., Tucson, AZ 85721, USA*
[2]*National Radio Astronomy Observatory, Socorro, NM 87801, USA*
[3]*European Southern Observatory, Karl-Schwarzschild-Strae 2, D-85748 Garching bei München, Germany*
[4]*Center for Astrophysics and Space Astronomy, University of Colorado, Boulder, CO 80309, USA*

Accepted 2017 November 17. Received 2017 November 14; in original form 2017 July 14

ABSTRACT

We present Atacama Large Millimeter Array (ALMA) observations of ^{12}CO 2–1 emission from circumstellar material around the massive star Eta Carinae (η Car). These observations reveal new structural details about the cool equatorial torus located ∼4000 au from the star. The CO torus is not a complete azimuthal loop, but rather, is missing its near side, which appears to have been cleared away. The missing material matches the direction of apastron in the eccentric binary system, making it likely that η Car's companion played an important role in disrupting portions of the torus soon after ejection. Molecular gas seen in ALMA data aligns well with the cool dust around η Car previously observed in mid-infrared (IR) maps, whereas hot dust resides at the inner surface of the molecular torus. The CO also coincides with the spatial and velocity structure of near-IR H_2 emission. Together, these suggest that the CO torus seen by ALMA is actually the pinched waist of the Homunculus polar lobes, which glows brightly because it is close to the star and warmer than the poles. The near side of the torus appears to be a blowout, associated with fragmented equatorial ejecta. We discuss implications for the origin of various features north-west of the star. CO emission from the main torus implies a total gas mass in the range of 0.2–1 $M_\odot$ (possibly up to 5 $M_\odot$ or more, although with questionable assumptions). Deeper observations are needed to constrain CO emission from the cool polar lobes.

Key words: circumstellar matter – stars: evolution – stars: winds, outflows.

1 INTRODUCTION

The Homunculus around the massive binary star Eta Carinae (η Car) is a striking example of a bipolar circumstellar nebula with a tightly pinched waist (see Smith 2012, for a recent overview). It serves as a prototypical object in ongoing attempts to understand the shaping of bipolar nebulae, and their physical origin from close binary systems or rapidly rotating stars (Frank 1999). It is perhaps most recognizable from stunning visible-wavelength images with the *Hubble Space Telescope* (*HST*) that show the complex clumpy structure of the dust shell (Morse et al. 1998), which unlike most ionized planetary nebulae, is seen primarily in reflected light at visible wavelengths. However, many clues about its structure and physical properties come from longer wavelengths where the nebula becomes transparent.

The dust shell around the star absorbs much of the star's tremendous luminosity and reradiates that energy in the infrared (IR), making the Homunculus around η Car one of the brightest extrasolar sources in the sky at thermal IR wavelengths (Neugebauer & Westphal 1968; Westphal & Neugebauer 1969). This made it a favourite target for early ground-based mid-IR observations, with repeated study spanning several decades as resolution and sensitivity improved (Gehrz et al. 1973; Robinson, Hyland & Thomas 1973; Sutton, Becklin & Neugebauer 1974; Aitken & Jones 1975; Apruzese et al. 1975; Joyce 1975; Andriesse, Donn & Viotti 1978; Mitchell et al. 1978; Hyland et al. 1979; Chelli, Perrier & Biraud 1983; Mitchell et al. 1983; Bensammer et al. 1985; Hackwell, Gehrz & Grasdalen 1986; Robinson et al. 1987; Russel 1987; Allen 1989; Smith et al. 1995, 2003; Smith, Gehrz & Krautter 1998; Morris et al. 1999; Polomski et al. 1999; Pantin & Le Mignant 2000; Hony et al. 2001; Smith 2002; Chesneau et al. 2005). Most of these showed an inner structure that was elongated perpendicular to the bipolar axis, often interpreted as a limb-brightened equatorial torus. Many of these authors supposed that such a dense equatorial torus

★ E-mail: nathans@as.arizona.edu
† Jansky Fellow.

might have been the agent that pinched the waist of the nebula, as seen in numerical simulations (Frank, Balick & Davidson 1995; Dwarkadas & Balick 1998; Frank, Ryu & Davidson 1998; Langer, Garcia-Segura & Mac Low 1999). The caps of the polar lobes are very dense and massive (Smith et al. 2003; Smith 2006), while the side walls and equatorial parts of the Homunculus are relatively transparent (Davidson et al. 2001; Smith 2002, 2006), so it would be difficult to make such a model work unless there is a large-mass reservoir of cold gas hidden in dense equatorial regions. While mid-IR emission traces warm dust heated by direct radiation from the central star, shielded dense gas could be cold and might be revealed by molecular emission at longer wavelengths.

Compared to the long history of studying its IR emission, molecular gas in the circumstellar nebula of η Car was detected fairly recently. Early surveys of CO in the Carina Nebula did not detect CO line emission from η Car itself (Cox et al. 1995). The first reported detection of molecules in the Homunculus arose via its near-IR emission from H_2 in several lines around 2 μm (Smith & Davidson 2001; Smith 2002). This H_2 emission traced very dense and very thin walls of the polar lobes of the Homunculus (Smith 2002, 2004, 2006; Smith & Ferland 2007), but was not seen from the equatorial ejecta except at the pinched waist of the polar lobes. Absorption from H_2 and several diatomic molecules like CH and OH was detected in UV spectroscopy of η Car obtained with *HST*, where the radial velocity and narrow line width indicated that this molecular gas was located in the thin walls of the south-east (SE) polar lobe (Nielsen, Gull & Viera Kober 2005; Verner et al. 2005). The first report of a polyatomic molecule was ammonia via the NH_3 $(J, K) = (3,3)$ inversion transition (Smith et al. 2006), although we note that Loinard (private communication) suggests that this line may actually be H recombination. Several additional molecules have since been detected via single-dish observations from the inner regions of the Homunculus (Loinard et al. 2012, 2016; Morris et al. 2017), and have also been attributed to the dusty torus seen in the IR. CO emission has also been detected in the circumstellar environments of other luminous blue variables (LBVs), including AG Carinae and HR Carinae (McGregor, Hillier & Hyland 1988; Nota et al. 2002). The total molecular gas mass around AG Car was estimated to be roughly 3 $M_\odot$, thought to reside mostly in an equatorial belt (Nota et al. 2002). In η Car, the H_2 emission is located mostly in the walls and caps of the two large polar lobes, but the density structure of the molecular gas located in equatorial regions, and its possible association with the IR torus, has remained uncertain.

Here, we present new Atacama Large Millimeter Array (ALMA) observations in the 230.5 GHz (1.3 mm) ^{12}CO 2–1 line obtained with an angular resolution of roughly 1 arcsec. These observations clearly delineate the spatial relationship between the densest molecular gas in the Homunculus as compared to the dusty IR torus and the thin walls of the polar lobes. We present the new observations in Section 2, and make various comparisons to spatially resolved optical and IR data in Section 3.

2 OBSERVATIONS

ALMA observations of η Car in Band 6 (1.3 mm) were taken as part of programme 2013.1.00661.S. Two scheduling blocks were executed on 2015 January 29 and 2015 April 3. The observations covered four basebands: 215.7–217.6 GHz, 217.6–219.5 GHz, 229.6–231.5 GHz, and 231.6–233.5 GHz. The velocity resolution achieved was 1.3 km s^{-1} (976 kHz). Data reduction was performed using the CASA pipeline version 4.2.2 r30986, and we used the QA2-produced visibilities and images. The continuum emission was fitted and subtracted. Here, we concentrate on the 230.5 GHz line of ^{12}CO 2–1. For the ^{12}CO 2–1 line, the RMS achieved was 7.2 mJy per 3 km s^{-1} channel in a 1.3 arcsec × 0.99 arcsec (P.A. = 67°) beam. Images were produced with Briggs weighting using a robust factor 0.5 and a cell size of 0.2 arcsec.

Fig. 1 shows maps of the peak CO emission (Fig. 1a) and the integrated line flux or zeroth moment of the CO emission (Fig. 1b). Panels (c) and (d) show the same contours of line flux from Fig. 1(b), but superposed on images of the mid-IR 8.8 μm and 18 μm optical depth maps, which show the relatively hot and cool mid-IR dust column density, respectively (from Smith et al. 2003). Fig. 2 shows a position–velocity diagram of the CO emission, and compares it to high-resolution near-IR spectra of near-IR H_2 emission (Smith 2004, 2006). Fig. 3 shows the same peak and line flux contours (from Figs 1a and b) superposed on a near-UV *HST* image of the Homunculus, for reference.

3 RESULTS AND DISCUSSION

3.1 The CO and IR torus

Images of the peak ^{12}CO emission and the integrated line flux (Figs 1a and b, respectively), show a clumpy ring-like structure, with an appearance that is very reminiscent of the IR torus structure in the core of the Homunculus, as discussed in the Introduction section. While these two maps trace the same basic structure, there are subtle differences due to the velocities over which the emission is dispersed. The apparent ring seen on the sky is indeed consistent with an expanding torus in the equatorial plane of the Homunculus, because it is redshifted to the SE and blueshifted to the north-west (NW). This gives an orientation perpendicular to the expansion of the polar lobes, consistent with expansion in the equator. Correcting for inclination, the radial expansion of this torus is 100–200 km s^{-1} (see below).

This torus, however, is not a smooth and azimuthally complete ring surrounding the star. The brightness structure reveals a handful of large condensations, with a pronounced wide gap in the ring or torus on the blueshifted NW side. In both the peak and integrated flux maps, the torus exhibits a 'C' shape, with the opening toward the NW. The integrated flux map gives the impression that the CO mass is concentrated on the redshifted SE side of the torus, especially apparent in Fig. 1(b). The clumpy and broken structure of this torus is remarkably similar, qualitatively, to the clumpy 'C'-shaped density distribution in the ionized ring nebula around the massive contact binary RY Scuti (Smith et al. 2002b). The strong departure from azimuthal symmetry in the CO torus around η Car may be extremely important for understanding the observed structure and origin of the Homunculus, as discussed more below.

The initial impression that the CO torus is reminiscent of the IR torus discussed in decades past is accurate. In fact, they have roughly the same size and structure. Figs 1(c) and (d) show the CO line flux contours superposed on mid-IR optical depth maps of the relatively warm (200–250 K) and cool (140 K) dust (Smith et al. 2002a, 2003). The clumpy IR torus shows good spatial correspondence with the CO torus in terms of a spatial structure; they should not match in the brightness distribution, since the CO map is flux and the IR maps are optical depth. (Note that maps of the IR optical depth essentially trace the dust mass column at different temperatures, rather than the brightness distribution. The central core region of the Homunculus is brighter at all IR wavelengths, because that is where the dust is hottest.)

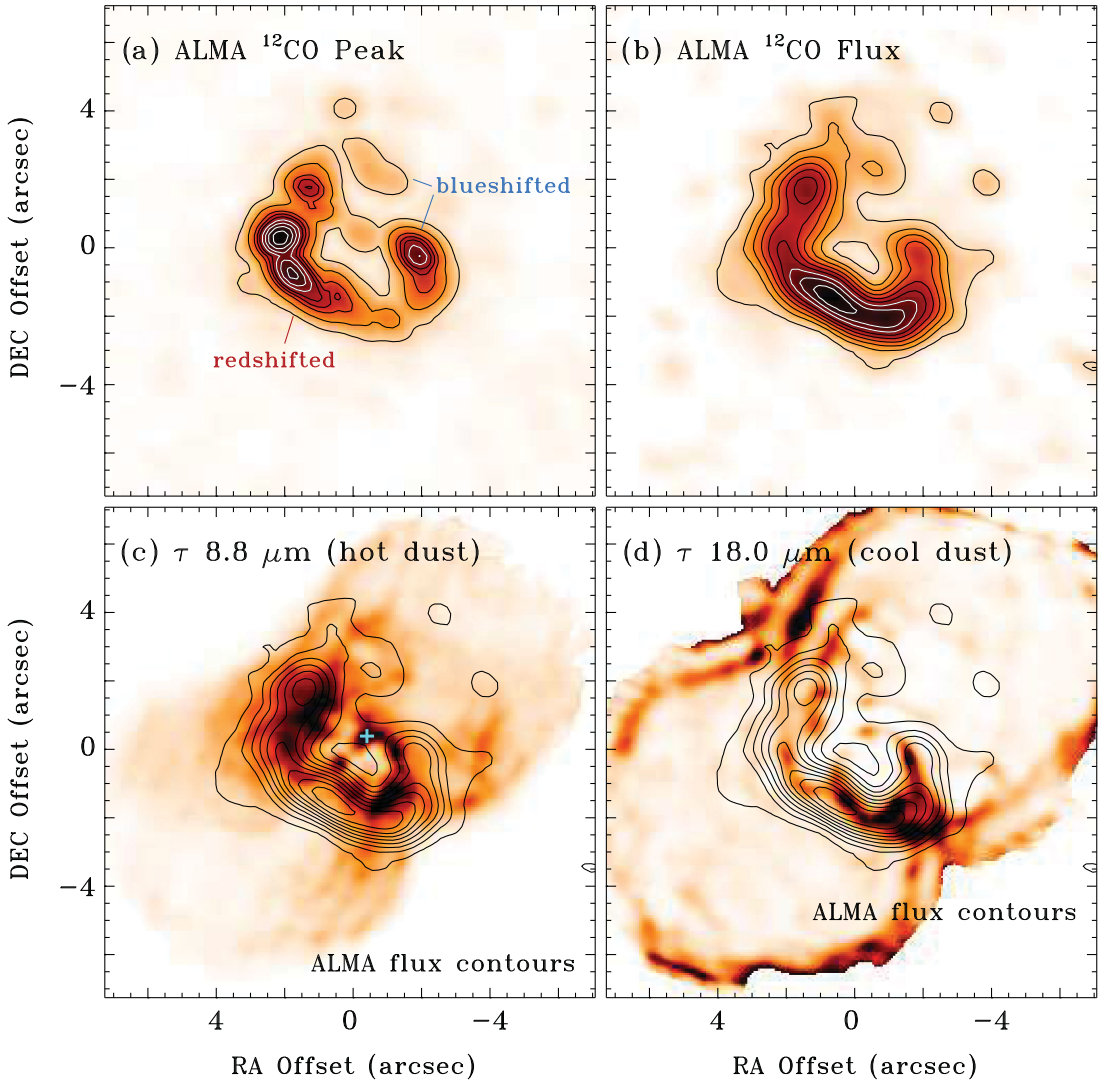

Figure 1. The top two panels show maps of the peak emission (a) and zeroth moment or integrated line flux (b) from the ALMA ^{12}CO 2–1 data cube. RA and Dec. offsets are relative to the star, for which the registration uncertainty is about 0.5 arcsec. Contours in panel (a) are at 10, 20, 30, 35, 40, 45, 50, 55, and 60 mJy. Contours in (b) are at 200, 400, 600, 800, 1000, 1200, 1400, 1600, and 1800 mJy km s^{-1}. The Jy to K conversion factor is 18.1 Jy K^{-1}, using a 1.28 arcsec × 0.99 arcsec beam at P.A. = 67° at 230.5 GHz. The contours from (b) are superposed on the two images in the bottom panels. These images show the 8.8 μm optical depth (essentially the column density of hot 200–400 K dust) in panel (c), and the 18 μm optical depth (essentially the column density of cooler 100–200 K dust) in panel (d). More details on the IR dust maps can be found in Smith et al. (2002a) and Smith et al. (2003). The blue '+' in panel (c) marks the hot NW dust condensation discussed in the text.

Both the spatially resolved dust temperature and IR emission-lines indicated a stratified double-shell structure in the Homunculus, with an inner zone of hotter dust and low-ionization atomic emission lines, and with a thin outer zone of cooler dust and H_2 emission (Smith 2002, 2006; Smith et al. 2003). The spatially resolved CO emission in our ALMA data arises from the outer of these two zones. Compared to the hot dust (traced by 8.8 μm optical depth), CO peaks at somewhat larger separation from the star, about 1 arcsec outside the 8.8 μm optical depth peak (Fig. 1c). However, the CO structures match well with the locations of several peaks in the 18 μm optical depth map (cooler dust; Fig. 1d). This is expected if the CO resides primarily in the walls of the polar lobes of the Homunculus, like H_2, because the thin walls are known to have a stratified temperature and density structure (Smith et al. 2003; Smith 2006; Smith & Ferland 2007). The spatial offset between the locations of the warmest dust and the CO is only about 0.5–1 arcsec, comparable to the thickness of the walls of the polar lobes themselves (Smith 2006). The hotter dust seen in the 8.8 μm emission traces a thin skin on the inside walls of the hollow polar lobes exposed to direct starlight, whereas the cooler dust and CO are shielded by the dense walls of the polar lobes and reside at slightly larger distances from the star.

Located within the gap in the torus (the opening of the 'C') to the NW of the star, there is a feature that shows a peak in the column of hot dust (in Fig. 1c), but that is much weaker in the cool dust and CO maps. This is a particularly noteworthy location, and is marked with a blue '+' in Fig. 1(c). It traces a complex of dust knots that marks the peak brightness in mid-IR images of the Homunculus, because there is a complex of dusty knots close to the star where the dust is heated to high temperatures, and where the inside edges of these dust clumps are ionized by UV radiation. Some of the brightest of these ionized knots are known as the 'Weigelt knots' (Weigelt

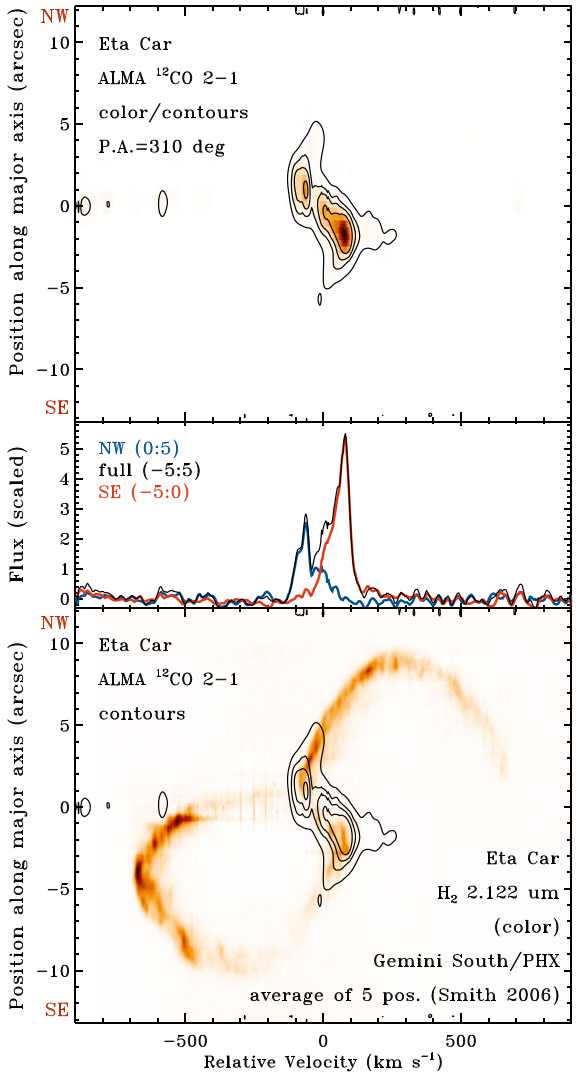

Figure 2. Top: position–velocity diagram of the ALMA ^{12}CO 2–1 data with the position running along the major axis of the Homunculus at P.A. = −50°, integrated over a spatial width of 5 arcsec (across the width of the 'torus'). Middle: integrated spectrum of the CO emission. The black line is emission from the full torus integrated over −5 to +5 arcsec along the position axis in the top panel, the blue line is the blueshifted NW side of the torus integrated over 0 to +5 arcsec, and the red line is the redshifted SE part of the torus integrated over −5 to 0 arcsec. Bottom: same contours from the top panel, but superposed on the near-IR H_2 emission from the Homunculus, taken with the Phoenix spectrograph on Gemini South. This is the average of several slits oriented along the same position angle, from Smith (2006).

& Ebersberger 1986; Weigelt et al. 1995), which have received much observational attention, although images show several other knots in the vicinity (Smith et al. 2004a; Chesneau et al. 2005; Gull et al. 2016). This dust feature is found in what is otherwise a gap in the CO and cool dust torus – yet this clump appears to have remained. Based on its structure, different temperature and column density, and kinematic evidence, we suspect that its location as part of the hot dust torus may be misleading, and that it may actually have a different origin, as discussed later.

Excluding this hot dust immediately NW of the star, the wide gap on the NW side of the torus is especially apparent in CO emission and the cool dust optical depth map in Fig. 1(d). These maps create the impression that this portion of the torus in the blueshifted side has suffered a blowout, as if something has disrupted the torus in this direction. Interestingly, this is a special direction in the η Car system, as discussed later. First, we discuss the kinematic structure of the CO emission detected by ALMA.

3.2 Near-IR H_2 emission and kinematic structure

In the previous section, a comparison of the new CO emission to the previously known dusty IR torus gave the impression that these two are closely related. The structure in images suggested that, like the IR torus, the CO emission traces material in the thin walls of the Homunculus, which is brightest in the pinched waist near the equator.

This interpretation is supported by the kinematics. Fig. 2 (top) shows a position–velocity diagram with the positional coordinate along the major axis of the Homunculus, and with the flux integrated in the direction perpendicular to the polar axis. This indicates that the CO emission has a flattened distribution, elongated perpendicular to the polar axis, in an expanding equatorial torus.

Fig. 2 (bottom) compares the kinematics of CO seen by ALMA to the kinematics of molecular hydrogen, as seen in high-resolution spectra of the Homunculus in the 2.122 μm H_2 line (Smith 2004, 2006). On the redshifted side of the CO torus (and toward negative positional offsets in Fig. 1), where the CO emission is brightest and where the CO torus traces the IR torus (see above), the kinematic structure of the CO emission overlaps perfectly with the near-IR H_2 emission. This confirms the conclusion from comparing the CO and IR maps (see above) that the CO emission seen by ALMA is not a more extended disc structure separate from the Homunculus, but is in fact just the molecular gas in the thin walls of the polar lobes that are pinched at the equator. The spatial coincidence of the spatially resolved CO emission with both the cool dust and H_2 emission from the outer shell of the Homunculus walls indicates that the CO is a good tracer of the cooler, dense, shielded zones in the Homunculus walls where most of the mass resides (Smith & Ferland 2007). The CO is not limited to a thin skin on the inner surface of these walls of the Homunculus (where the hotter dust resides), and so it is likely that the CO 2–1 emission is tracing the regions with most of the mass.

The redshifted peak of the torus has a radial velocity of about +81 km s^{-1}, which corresponds to an expansion speed away from the star (correcting for an inclination of $i = 41°$; Smith 2006) of about 123 km s^{-1}. This is the same as the H_2 emission, as noted above. Morris et al. (2017) noted a similar velocity range for far-IR transitions of CO, which suggests again that both the H_2 and CO emission lines are probably optically thin and are tracing the same gas. This makes it unlikely that a huge reservoir of cold, shielded mass would be undetected in our ALMA data. The projected radius of the torus is ∼1.9 arcsec, or a radial distance from the star of 4400 au. This translates to a kinematic age of around 170 (±15) yr, indicating that the CO torus was ejected during the Great Eruption along with the rest of the Homunculus (Morse et al. 2001; Smith 2017b). The CO emission is not tracing an older, pre-existing disc as advocated by Morris et al. (1999). The reason that the CO appears only as a torus in the flux maps is probably just because this gas is the closest to the star, and so is the warmest and brightest of the CO emission. We suspect that deeper CO observations are needed to detect CO at larger Doppler shifts in the polar regions of the lobes, where H_2 is seen.

On the blueshifted side of the CO emission distribution, which is fainter (and located toward positive spatial offsets), most of the

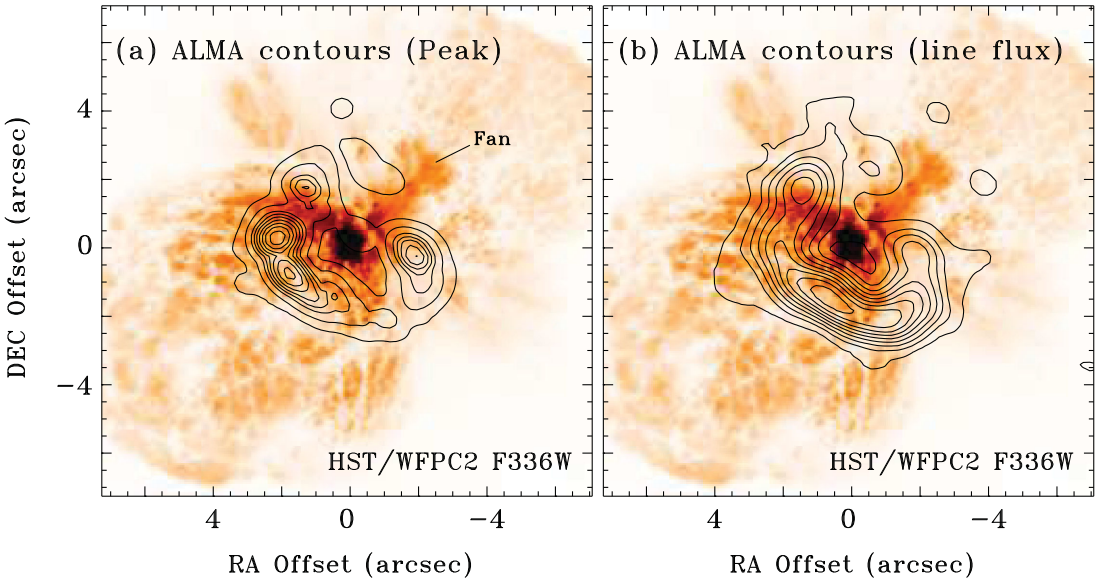

Figure 3. These are the same ^{12}CO contours from Figs 1(a) and (b) (peak emission and zeroth moment, respectively), but superposed on the *HST*/WFPC2 *F336W* image from Morse et al. (1998).

CO also overlaps with the near-IR H_2 emission from the NW polar lobe walls in Fig. 2. There are, however, some fainter CO clumps on the NW/blueshifted side of the torus that are farther from the star, fainter, and more ragged; although these do not show up in the integrated position–velocity diagram in Fig. 2, they can be seen in Fig. 1. CO structures appear to be less dense and more wispy to the NW direction, as compared to the rest of the torus. Altogether, the IR and CO images give the impression that the NW side of the torus has been disrupted or blown out, with thin clumps pushed to larger distances from the star as something broke through the torus. This may be related to many of the interesting and peculiar aspects of the equatorial ejecta to the NW of the star that have been noted by many authors, as discussed in the next section.

3.3 The 'blowout' on the near side of the torus, and its relation to the equatorial ejecta

In the two previous sections, we noted how the observed CO structure in combination with other data gives the impression that the dense equatorial material around η Car has two key aspects. The first main component is an incomplete expanding torus with a 'C'-shaped density distribution, where the NW/blueshifted side of the expanding torus is missing. This torus corresponds to the thin, cold walls of the Homunculus that are pinched at the waist, where their proximity to the star makes them much brighter than the rest of the nebula. The second feature is a relative paucity of CO emission on the blueshifted side of the equator corresponding to the gap in the 'C'-shaped density distribution, which might be a 'blowout' where molecular gas to the NW of the star has been pushed out or diverted, and takes on a much more ragged or whispy distribution.

Fig. 3 shows the CO contours superposed on an optical/near-UV image from *HST* (Morse et al. 1998), showing the reflection nebula and especially the equatorial ejecta. While we of course cannot see the far side of the equatorial region at visible wavelengths because of obscuration, it is clear that on the near side, the faint CO features are pushed to larger radii than the rest of the CO/IR torus, coincident with the region of the peculiar equatorial ejecta. In fact, the CO emission a few arcseconds to the N and E of star corresponds to dark patches in the equatorial ejecta, which have been inferred to be regions of higher visual-wavelength extinction in the equatorial skirt based on multiwavelength optical/IR imaging (Smith, Gehrz & Krautter 1998, 1999; Smith et al. 2002a, 2003).

The gap to the NW may hold vital clues and may have important implications for understanding the time sequence of mass ejection that produced the Homunculus, because the NW direction is special. In the central binary system, the NW corresponds to the direction of apastron of the very eccentric orbit (Gull et al. 2009; Madura et al. 2012), where η Car's hot companion spends most of its time during the 5.5 yr cycle (see Fig. 4). The opening of the colliding-wind shock cone therefore points in this direction most of the time. There are several notable nebular features (see Fig. 4) that are all associated with this direction in the equatorial plane of the Homunculus.

(i) *The Weigelt knots and NW dust complex.* This is a series of dense condensations located 0.1–0.5 arcsec from the central star that were resolved by early speckle interferometry techniques (Weigelt & Ebersberger 1986; Weigelt et al. 1995) and in high-resolution IR images (Chesneau et al. 2005). These nebular knots have very strong narrow atomic emission lines throughout the UV, optical, and near-IR spectrum (Davidson et al. 1995, 1997; Smith 2002; Smith et al. 2004a; Hartman et al. 2005). Proper motions show that the Weigelt knots and some of the other features are younger than the polar lobes (Dorland, Currie & Hajian 2004; Smith et al. 2004a), having been ejected in the 1890 eruption or later.

(ii) *The bright 'Fan' to the NW of the star*. This feature appears to squirt out through the gap in the torus (see Fig. 3a). In fact, it has been noted previously that the Fan is an optical illusion (Smith et al. 1998, 1999, 2003; Davidson et al. 2001; Smith 2012). Rather than a density structure, it is bright because it is a patch of lower extinction (i.e. a hole, rather than a dense clump in the equator) allowing scattered light from the NW lobe to pass through the equatorial plane. This is consistent with the paucity of CO emission at this location.

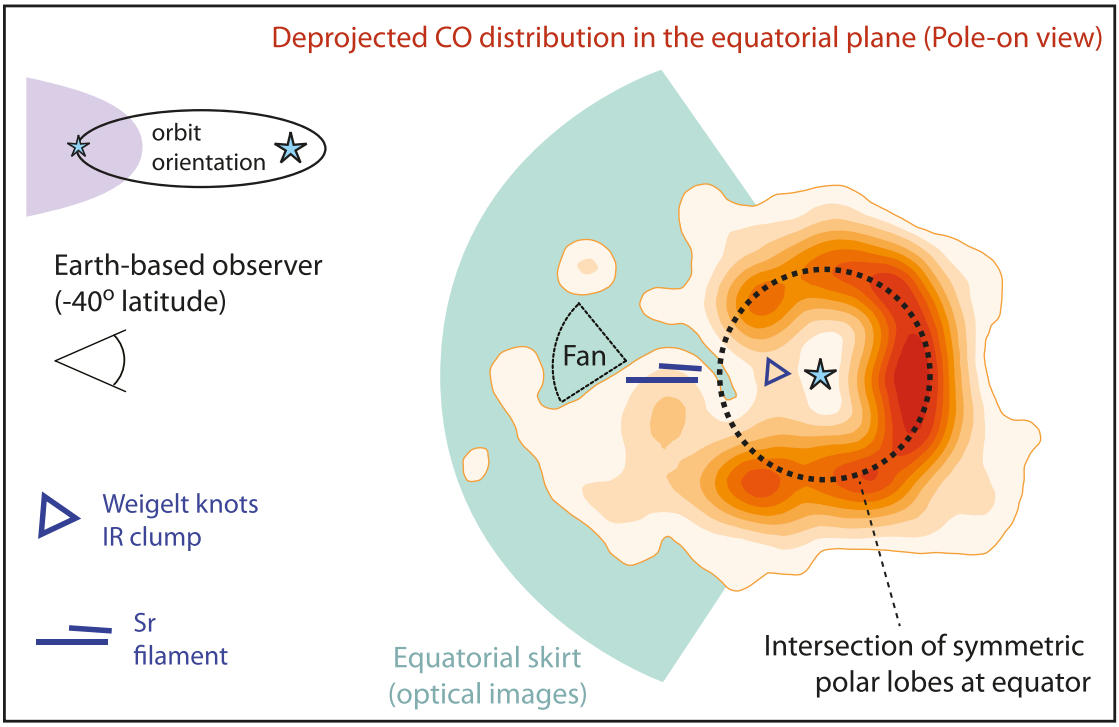

Figure 4. Sketch of the equatorial geometry. The red/orange contours correspond to the ALMA ^{12}CO flux in an image, deprojected for an inclination angle of $i \simeq 40^{\circ}$, corresponding to the tilt of the equatorial plane of the Homunculus from the plane of the sky (Smith 2006). This is an approximation of a 'pole-on' view of the CO as seen by an observer in the SE polar lobe. The location of an Earth-based observer (who would be 40° out of this image plane) is at left. Other features are drawn to represent the extent of the visible equatorial skirt (green pie wedge), the location of the strontium filament (blue hash marks) and the complex of dusty knots that includes the Weigelt knots (blue triangle). The location of the 'Fan' is also noted. The approximate orientation of the central binary system's orbit is shown at the upper left for reference (with the purple zone representing the colliding-wind shock cone opening), where the direction of the secondary at apastron is to the left.

(iii) *Several thin filaments at the base of the Fan; the so-called 'strontium filament' and others.* These are a collection of several thin filaments located 0.5–2.5 arcsec NW of the star. They show peculiar low excitation, with strong emission from unusual forbidden lines including [Sr II] and many other low-ionization metal lines (Hartman et al. 2004; Bautista et al. 2006, 2009). Radial velocities show peculiar kinematics that do not match simple expectations for the equator of the Homunculus, either corresponding to a range of ejection dates before and after the Great Eruption, or instead, a range of latitudes out of the equator (Zethson et al. 1999; Davidson et al. 2001; Smith 2002).

(iv) *Extended equatorial emission features in He I and other lines.* Emission from hot equatorial gas that may have multiple ages (or multiple latitudes offset from the equator) is seen in lines such as He I λ10 30 in front of the NW polar lobe (Smith 2002, 2008; Teodoro et al. 2008). Curiously, these features are not seen in H I recombination lines or [Fe II] lines like most of the other extended ejecta outside the Homunculus. This emission appears to be projected outward from the gap in the CO torus.

(v) *The equatorial skirt is one-sided.* The collection of dusty clumps, streaks, bright spots, and streamers that collectively make up the 'equatorial skirt' is prominent in near-UV and visual-wavelength images in scattered light (Fig. 3). They seem to fade and then disappear as we move to longer wavelengths in the near-IR and mid-IR, however, suggesting that they are mostly scattered light illumination effects (i.e. searchlight beams escaping the core) rather than dense structures in a disc (Smith et al. 1999, 2002a, 2003; Smith 2002, 2006). Zethson et al. (1999) pointed out that the equatorial skirt is very lopsided, concentrated on our side of the Homunculus. If one fits an ellipse to the outer boundary of the skirt and centres this ellipse on the star, it is evident that the parts of the skirt on the far side of the Homunculus are missing (see their fig. 1). If one fits an ellipse to the observed boundaries of the skirt, the centre of such an ellipse is more than 1 arcsec NW of the star (again, see fig. 1 in Zethson et al. 1999). Instead of a full azimuthally symmetric disc (like a 'tutu' at the waist of the Homunculus), the observable equatorial skirt is more like a wide pie wedge; this is represented by the blue–green area in Fig. 4. This makes sense in light of the new ALMA data that show a pronounced gap in the NW side of the inner IR/CO torus. This gap may allow visible and near-UV light to escape preferentially in these directions to illuminate the skirt.

This preferred direction for all these equatorial features that point in our direction would seem to violate the Copernican principle, unless they are all physically related to the orientation of the orbit of the central eccentric binary system (which, by chance, does happen to point toward us in the equatorial plane). As noted earlier, the $e \simeq 0.9$ orbit ($a = 15$ au) of the central binary observed at the present epoch has the secondary star located to the NW of the primary, so that the major axis of the orbit points out toward the NW in the equatorial plane (Madura et al. 2012).

There are key ways in which the orientation of the eccentric orbit may have played a role in shaping the ejecta. First, at early times during the 19th century eruption, the presence of the massive companion star in its orbit may have actually disrupted the density structure of the torus. At the earliest phases after ejection of the Homunculus in the late 1840s (Morse et al. 2001; Smith 2017b),

the size of the torus may have been comparable to the size of the orbit, and when at apastron, the companion may have actually ripped through that torus and punched a hole. Later, in post-eruption times, any post-eruption wind would have had an easier time escaping through this hole.[1] In particular, with the secondary spending most of its time at apastron, the shock cone of the interacting winds is aimed in the same direction as the gap in the torus. This pre-existing gap may have funnelled the fast wind and UV radiation of the companion out in this direction. Moreover, dust that was formed in the post-shock cooling zones of the colliding-wind shock cone (Smith 2010) would travel downstream preferentially in the NW direction, out through this hole.

As noted earlier, we suspect that the complex of dust clumps that comprises the Weigelt knots (and related features in the hot dust peak NW of the star; Chesneau et al. 2005) may be from this type of dust formation in the post-eruption colliding winds that piles up at this location. As such, the peak of hot dust immediately NW of the star (Fig. 1c) may actually be unrelated to the rest of the cool dust and the molecular torus. In fact, its location would place it inside the ring that would define the location of the torus at the intersection of the two polar lobes (Fig. 4). Moreover, we know that this feature is younger than the rest of the Homunculus anyway, as noted above (Dorland et al. 2004; Smith et al. 2004a). In a similar vein, elongated features like the Sr filament or other structures in front of the NW polar lobe may be caused by ablation from this post-eruption dust ejection that gets entrained by the faster wind escaping in this direction. The peculiar excitation of the Sr filament may be due partly to the fact that it resides in the shadow of the hot dust clumps closer to the star.

The pronounced gap in the density structure on the blue side of the torus and the associated blowout is also interesting in relation to the structure of the polar lobes. Specifically, the polar lobes are very nearly axisymmetric – their geometry *does not* exhibit blowouts on the side facing Earth (Davidson et al. 2001; Smith 2006). Why not? If the torus is the thing that constricted the waist of the Homunculus to form the bipolar structure, then presumably a much lower density in the torus in one direction would give it much less inertia with which to pinch the waist there. We must conclude that either (1) the IR/CO torus is not the agent that constricted the waist of the lobes, and the bipolar shape has an origin in the ejection from the star itself (Smith et al. 2003; Smith 2006), or (2) the disruption of the NW portion of the torus by the companion happened after the Homunculus polar lobes were already shaped by it at very early times, and at radii smaller than the apastron distance of the companion (or both). We do not propose a clear answer here, but this is an important consideration for any explanation for the shaping of the nebula that invokes a binary (or triple) system.

3.4 Mass estimate from CO data

As noted above, the CO emission coincides with the cooler dust in the very dense walls of the polar lobes, where we expect the gas and dust temperature (140 K) to be similar. The peak CO brightness temperature we observe is 12.4 K, implying either that the CO is very optically thin, or if it is optically thick, that it most likely has a filling factor less than 0.1 in our beam. Averaged over a projected area on the sky of 450 arcsec^2 (0.056 pc^2 at the 2.3 kpc distance of η Car; Smith 2006), we measure an average integrated surface brightness in ^{12}CO 2–1 emission of 26 ($\pm$0.4) K km s^{-1} in our ALMA data (with a peak value of 397 K km s^{-1}). Converting this to a mass of molecular gas around η Car is tricky. One might estimate the total molecular hydrogen gas mass from the integrated CO 2–1 emission using a standard X-factor approach, assuming the 'average' X-factor from Bolatto, Wolfire & Leroy (2013), where $X_{\rm CO} = 2\times\ 10^{20}$ cm^{-2} (K km s^{-1})$^{-1}$. This is the X-factor for ^{12}CO (1–0); the (2–1) X-factor is similar, perhaps 80 per cent of the 1–0 value (Leroy et al. 2013), which would lower our value a little. Using this assumption, the corresponding total inferred molecular hydrogen mass in the area of the torus would be about 5 M$_\odot$ or higher depending on the relative CNO abundance. However, this value uses the standard X-factor intended for average measurements of a typical spiral galaxy, which is probably inapplicable here.

The high density and intense radiation field in the Homunculus are, to say the least, very different from typical galaxy interstellar medium (ISM) conditions, so the appropriate X-factor to use here may be different. For example, for the dense and warm ISM in starburst galaxies, Bolatto et al. (2013) suggest using $X_{\rm CO} = 0.4\times$ 10^{20} cm^{-2} (K km s^{-1})$^{-1}$, which is a factor of five lower, implying a total mass for the torus around η Car of 1 M$_\odot$ (or somewhat more depending, again, on the relative CNO abundance). In any case, the correct X-factor to use is highly uncertain. An LTE optically thin analysis leads to a total CO mass of roughly $5.9\times\ 10^{-4}$ M$_\odot$. Converting this to a total molecular H gas mass assuming a standard CO/H$_2$ number ratio of 10^{-4} gives roughly 0.42 M$_\odot$. On the other hand, Nota et al. (2002) estimated a CO/H$_2$ mass ratio of $2.3\times$ 10^{-3} (number ratio of $1.6\times\ 10^{-4}$) in the dense, N-enriched, and irradiated circumstellar environment of the LBV star AG Carinae. Using this latter conversion would imply a lower total molecular gas mass in η Car's torus of only 0.26 M$_\odot$. Clearly, the dominant uncertainty here is in the appropriate conversion of CO to H$_2$, with implied total H$_2$ masses ranging from 0.2 to 5 M$_\odot$ depending on the adopted conversion. Consequently, we infer $\sim$1 M$_\odot$ as a very rough order-of-magnitude estimate for the total molecular gas mass of the CO torus seen in our ALMA data, although we acknowledge that further study including a multilevel analysis of CO is needed to understand the implications of the CO emission in this particular environment.

Detailed study of N-rich molecular chemistry in warm circumstellar material (CSM) near a luminous star is beyond the scope of this paper, but is needed before one can translate the CO measurements to a reliable mass. A total mass of as much as several M$_\odot$ in the equator is reasonably in line with what one expects for the equatorial portion of the Homunculus (Smith et al. 2003; Smith & Ferland 2007), which should have roughly 10–20 per cent of the total mass of the Homunculus. Although we detect some CO from the inner side walls of the polar lobes, much deeper observations are needed to investigate the mass in the fainter and cooler caps of the polar lobes.

3.5 One-sided equatorial mass ejection

Recent studies of Type IIn supernovae (SNe) have given some examples where the observed signatures of strong interaction with

[1] Note, however, that it seems unlikely that the directionality of the companion's wind (i.e. the opening of the colliding-wind shock cone) is the sole agent that shaped this gap, because the companion wind's momentum falls short by orders of magnitude. In order for the low-density wind to be able to shape the equatorial torus, the equatorial material would need a total mass far below 0.1 M$_\odot$. Roughly, 0.2 M$_\odot$ is the low end of values we estimate from CO emission below.

dense CSM show evidence of a blast wave interacting with an equatorial disc or torus. This is based on multiple-peaked line profiles at late times, polarization, or other evidence (Leonard et al. 2000; Hoffman et al. 2008; Levesque et al. 2014; Mauerhan et al. 2014; Smith, Mauerhan & Prieto 2014). In some cases, the mass distribution around the torus is thought to significantly break azimuthal symmetry. This presents an interesting mystery, because equatorial mass-loss from rotating stars or from close mass-transferring binaries should be azimuthally symmetric like the ring around SN 1987A. Some examples of such azimuthal asymmetry are SN 1998S (Leonard et al. 2000; Mauerhan & Smith 2012; Shivvers et al. 2015), SN 2010jl (Fransson et al. 2014), PTF11iqb (Smith et al. 2015), SN 2012ab (Bilinski et al. 2017), SN2013L (Andrews et al. 2017), and others. Episodic mass ejection and eccentric binaries have been invoked as possible explanations for some of these events.

The CO torus around η Car may provide us with a vivid pre-SN snapshot of this type of non-azimuthally symmetric CSM distribution. As such, it may give confirmation of the suspected influence of mass ejection in eccentric binary systems. Imagine that another few hundred years pass by. The fast polar lobes of the Homunculus will expand to very large distances, and will become optically thin and faint. The slower and denser equatorial torus seen in ALMA data presented here, however, will linger near the star (concentrated on one side), waiting to be hit by the eventual SN blast wave. When this finally happens, the collision with the denser redshifted side of the torus will have much more intense CSM interaction luminosity than the near side, which has been mostly blown out as noted above. As such, the resulting emission line profile from the interaction (i.e. H α) will not be a symmetric double-peaked line that we expect from a torus. Rather, the red peak will be much stronger, resembling observed cases of SNe like PTF11iqb (Smith et al. 2015). Interestingly, there is strong evidence that η Car has suffered mostly one-sided mass ejections in its past as well (Kiminki, Reiter & Smith 2016), although with a different orientation.

The total mass of dense molecular gas that we infer from the CO observations (very roughly, 0.2–5 $M_{\odot}$; see above) overlaps well with CSM mass estimates from SNe IIn with signs of strong CSM interaction (see Smith 2017a for a review). This would be the case if η Car explodes in the future after a long delay, and interacts primarily with its slow equatorial gas that remains in the vicinity of the star. Had it exploded a decade or so after the Great Eruption, the gas in the Homunculus polar lobes would have been much closer to the star and would have been hit by the SN right away, producing a superluminous Type II event. The asymmetry in that case would probably be much less pronounced, due to the high degree of axial symmetry in the polar lobes around η Car.

ACKNOWLEDGEMENTS

This paper makes use of the following ALMA data: ADS/JAO.ALMA#2013.1.00661.S. ALMA is a partnership of NSF (USA), ESO (representing its member states), and NINS (Japan), together with NRC (Canada), MOST and ASIAA (Taiwan), and KASI (Republic of Korea), in cooperation with the Republic of Chile. The Joint ALMA Observatory is operated by ESO, AUI/NRAO, and NAOJ. The National Radio Astronomy Observatory (NRAO) is a facility of the National Science Foundation (NSF) operated under cooperative agreement by Associated Universities, Inc. NS's research on Eta Carinae and eruptive massive stars was supported by NSF grants AST-1312221 and AST-1515559. Additional support for this work was provided by NASA grants AR-12618 and AR-14586 from the Space Telescope Science Institute, which is operated by the Association of Universities for Research in Astronomy, Inc. under NASA contract NAS 5-26555.

REFERENCES

Aitken D. K., Jones B., 1975, MNRAS, 172, 141
Allen D. A., 1989, MNRAS, 241, 195
Andrews J. E., Smith N, McCully C., Fox O. D., Valenti S., Howell D. A., 2017, MNRAS, 471, 4047
Andriesse C. D., Donn B. D., Viotti R., 1978, MNRAS, 185, 771
Apruzese J. P., 1975, ApJ, 196, 753
Bautista M. A., Hartman H., Gull T. R., Smith N., Lodders K., 2006, MNRAS, 370, 1991
Bautista M. A., Ballance C., Gull T. R., Hartman H., Lodders K., Martà-nez M., Melendez M., 2009, MNRAS, 393, 1503
Bensammar S., Letourneur N., Perrier F., Friedjung M., Viotti R., 1985, A&A, 146, L1
Bilinski C. et al., 2017, preprint (arXiv:1712.03370)
Bolatto A. D., Wolfire M., Leroy A. K., 2013, ARA&A, 51, 207
Chelli A., Perrier C., Biraud Y. G., 1983, A&A, 117, 199
Chesneau O. et al., 2005, A&A, 435, 104
Cox P., Mezger P. G., Sievers A., Najarro F., Bronfman L., Kreysa E., Haslam G., 1995, A&A, 297, 168
Davidson K., Ebbets D., Weigelt G., Humphreys R. M., Hajian A. R., Walborn N. R., Rosa M., 1995, AJ, 109, 1784
Davidson K. et al., 1997, AJ, 113, 335
Davidson K., Smith N., Gull T. R., Ishibashi K., Hillier D. J., 2001, AJ, 121, 1569
Dorland B. N., Currie D. G., Hajian A. R., 2004, AJ, 127, 1052
Dwarkadas V. V., Balick B., 1998, AJ, 116, 829
Frank A., 1999, New Astron. Rev., 43, 31
Frank A., Balick B., Davidson K., 1995, ApJ, 441, L77
Frank A., Ryu D., Davidson K., 1998, ApJ, 500, 291
Fransson C. et al., 2014, ApJ, 797, 118
Gehrz R. D., Ney E. P., Becklin E. E., Neugebauer G., 1973, Astrophys. Lett., 13, 89
Gull T. R. et al., 2009, MNRAS, 396, 1308
Gull T. R. et al., 2016, MNRAS, 462, 3196
Hackwell J. A., Gehrz R. D., Grasdalen G. L., 1986, ApJ, 311, 38
HST Eta Carinae Treasury Project TeamHartman H., Gull T., Johansson S., Smith N., 2004, A&A, 419, 215
Hartman H., Damineli A., Johansson S., Letokhov V. S., 2005, A&A, 436, 945
Hoffman J. L., Leonard D. C., Chornock R., Filippenko A. V., Barth A. J., Matheson T., 2008, ApJ, 688, 1186
Hony S. et al., 2001, A&A, 377, L1
Hyland A. R., Robinson G., Mitchell R. M., Thomas J. A., Becklin E. E., 1979, ApJ, 233, 145
Joyce R. R., 1975, PASP, 87, 917
Kiminki M. M., Reiter M., Smith N., 2016, MNRAS, 463, 845
Langer N., Garcia-Segura G., Mac Low M. M., 1999, ApJ, 520, L49
Leonard D. C., Filippenko A. V., Barth A. J., Matheson T., 2000, ApJ, 536, 239
Leroy A. K. et al., 2013, AJ, 146, 19
Levesque E. M., Stringfellow G. S., Ginsburg A. G., Bally J., Keeney B. A., 2014, AJ 147, 23
Loinard L., Menten K. M., Gusten R., Zapata L. A., Rodriguez L. F., 2012, ApJ, 749, L4
Loinard L., Kaminski T., Serra P., Menten K. M., Zapata L. A., Rodriguez L. F., 2016, ApJ, 833, 48
McGregor P. J., Hillier D. J., Hyland A. R., 1988, ApJ, 334, 639
Madura T. I., Gull T. R., Owocki S. P., Groh J. H., Okazaki A. T., Russell C. M. P., 2012, MNRAS, 420, 2064
Mauerhan J. C., Smith N., 2012, MNRAS, 424, 2659
Mauerhan J. C. et al., 2014, MNRAS, 442, 1166
Mitchell R. M., Robinson G., 1978, ApJ, 220, 841
Mitchell R. M., Robinson G., Hyland A. R., Jones T. J., 1983, ApJ, 271, 133

Morris P. W. et al., 1999, Nature, 402, 502
Morris P. W., Gull T. R., Hillier D. J., Barlow M. J., Royer P., Nielsen K., Black J., Swinyard B., 2017, ApJ, 842, 79
Morse J. A., Davidson K., Bally J., Ebbets D., Balick B., Frank A., 1998, AJ, 116, 2443
Morse J. A., Kellogg J. R., Bally J., Davidson K., Balick B., Ebbets D., 2001, ApJ, 548, L207
Neugebauer G., Westphal J. A., 1968, ApJ, 152, L89
Nielsen K. E., Gull T. R., Viera Kober G., 2005, ApJS, 157, 138
Nota A., Pasquali A., Marston A. P., Lamers H. J. G. L. M., Clampin M., Schulte-Ladbeck R. E., 2002, AJ, 124, 2920
Pantin E., Le-Mignant D., 2000, A&A, 355, 155
Polomski E., Telesco C. M., Pina R. K., Fisher R. S., 1999, AJ, 118, 2369
Robinson G., Hyland A. R., Thomas J. A., 1973, MNRAS, 161, 281
Robinson G., Mitchell R. M., Aitken D. K., Briggs G. P., Roche P. F., 1987, MNRAS, 227, 535
Russel R. W., Lynch D. K., Hackwell J. A., Rudy R. J., Rossano G. S., Castelaz M. W., 1987, ApJ, 321, 937
Shivvers I., Mauerhan J. C., Leonard D. C., Filippenko A. V., Fox O. D., 2015, ApJ, 806, 213
Smith N., 2002, MNRAS, 337, 1252
Smith N., 2004, MNRAS, 351, L15
Smith N., 2006, MNRAS, 644, 1151
Smith N., 2008, Nature, 455, 201
Smith N., 2010, MNRAS, 402, 145
Smith N., 2012, in Humphreys R. M., Davidson K., eds, Eta Carinae and the Supernova Impostors. Springer-Verlag, Berlin
Smith N., 2017a, in Alsabti A., Murdin P., eds, Interacting Supernovae: Types IIn and Ibn, Handbook of Supernovae, Vol 3, Springer, Cham
Smith N., 2017b, MNRAS, 471, 4465
Smith N., Davidson K., 2001, ApJ, 551, L101
Smith N., Ferland G. J., 2007, ApJ, 655, 911
Smith C. H., Aitken D. K., Moore T. J. T., Roche P. F., Puetter R. C., Pina R. K., 1995, MNRAS, 273, 354
Smith N., Gehrz R. D., Krautter J., 1998, AJ, 116, 1332
Smith N., Gehrz R. D., Krautter J., 1999, in Morse J. A., Humphreys R. M., Damineli A., eds, ASP Conf. Ser. Vol. 179, Eta Carinae at the Millenium. Astron. Soc. Pac., San Francisco, p. 31
Smith N., Gehrz R. D., Hinz P. M., Hoffmann W. F., Mamajek E. E., Meyer M. R., Hora J. L., 2002a, ApJ, 567, L77
Smith N., Gehrz R. D., Stahl O., Balick B., Kaufer A., 2002b, ApJ, 578, 464
Smith N., Gehrz R. D., Hinz P. M., Hoffmann W. F., Hora J. L., Mamajek E. E., Meyer M. R., 2003, AJ, 125, 1458
Smith N. et al., 2004, ApJ, 605, 405
Smith N., Brooks K. J., Koribalski B., Bally J., 2006, ApJ, 645, L41
Smith N., Mauerhan J. C., Prieto J. L., 2014, MNRAS, 438, 1191
Smith N. et al., 2015, MNRAS, 449, 1876
Sutton E., Becklin E. E., Neugebauer G., 1974, ApJ, 190, L69
Teodoro M., Damineli A., Sharp R. G., Groh J. H., Barbosa C. L., 2008, MNRAS, 387, 564
Verner E., Bruhweiler F., Nielsen K. E., Gull T. R., Viera kober G., Corcoran M. F., 2005, ApJ, 629, 1034
Weigelt G., Ebersberger J., 1986, A&A, 163, L5
Weigelt G. et al., 1995, Rev. Mexicana Astron. Astrofis. Ser. Conf., 2, 11
Westphal J. A., Neugebauer G., 1969, ApJ, 156, L45
Zethson T., Johansson S., Davidson K., Humphreys R. M., Ishibashi K., Ebbets D., 1999, A&A, 344, 211

This paper has been typeset from a TEX/LATEX file prepared by the author.